World Journal of Advanced Research and Reviews
eISSN: 2581-9615 CODEN (USA): WJARAI
Cross Ref DOI: 10.30574/wjarr
Journal homepage: https://wjarr.com/

(RESEARCH ARTICLE)

Check for updates

Isotherm, kinetics and thermodynamics of adsorption of Bisphenol A onto modified and unmodified corn cob: A comparative study

Nkechinyere Olivia Eze [1,*], Onyinye Nnenna Ogbonna [2] and Nnamdi Samuel [1]

[1] *Department of Industrial Chemistry, Ebonyi State University, Abakaliki, Ebonyi State, Nigeria.*
[2] *Department of Industrial Chemistry, Evangel University, Akaeze, Ebonyi State, Nigeria*

World Journal of Advanced Research and Reviews, 2025, 25(03), 1980-1993

Publication history: Received on 12 February 2025; revised on 23 March 2025; accepted on 26 March 2025

Article DOI: https://doi.org/10.30574/wjarr.2025.25.3.0914

Abstract

This study investigated the adsorption characteristics of bisphenol A (BPA) onto unmodified corn cob (UMCC) and hydrogen peroxide-modified corn cob (MCC) to evaluate their efficiency as adsorbents. The UMCC and MCC were synthesized using standard procedures, and characterized using SEM (Phenom Pro X) and FTIR (Cary 630 Agilent Technologies). Batch adsorption experiments were conducted to determine the effects varying contact time, adsorbent dosage, pH, temperature, and initial BPA concentration on the adsorbent performances. Scanning electron microscopy (SEM) images revealed that MCC had a more porous and irregular surface morphology than UMCC, contributing to its higher adsorption efficiency. The maximum BPA removal occurred at pH 6. Adsorption equilibrium was attained at contact time of 40 min at 86.25 and 60.30 % removal for both MCC and UMCC respectively. Adsorption also increased with increased temperature from 25 ^{0}C to 65 ^{0}C. Adsorption isotherms were analyzed using Langmuir, Freundlich, and Temkin models, with the Langmuir model providing the best fit. Kinetic studies using pseudo-first-order and pseudo-second-order, indicated that the pseudo-second-order model best described the adsorption process. Thermodynamic analysis (ΔG°, ΔH°, and ΔS°) confirmed that the adsorption was spontaneous and endothermic. These results suggest that corn cob biochar, particularly MCC, is a promising adsorbent for BPA removal from aqueous solutions.

Keywords: Bisphenol A; H_2O_2 modified corn cob; Unmodified corn cob; Adsorption isotherm; Kinetic; thermodynamic

* Corresponding author: Nkechinyere Olivia Eze

Graphical abstract

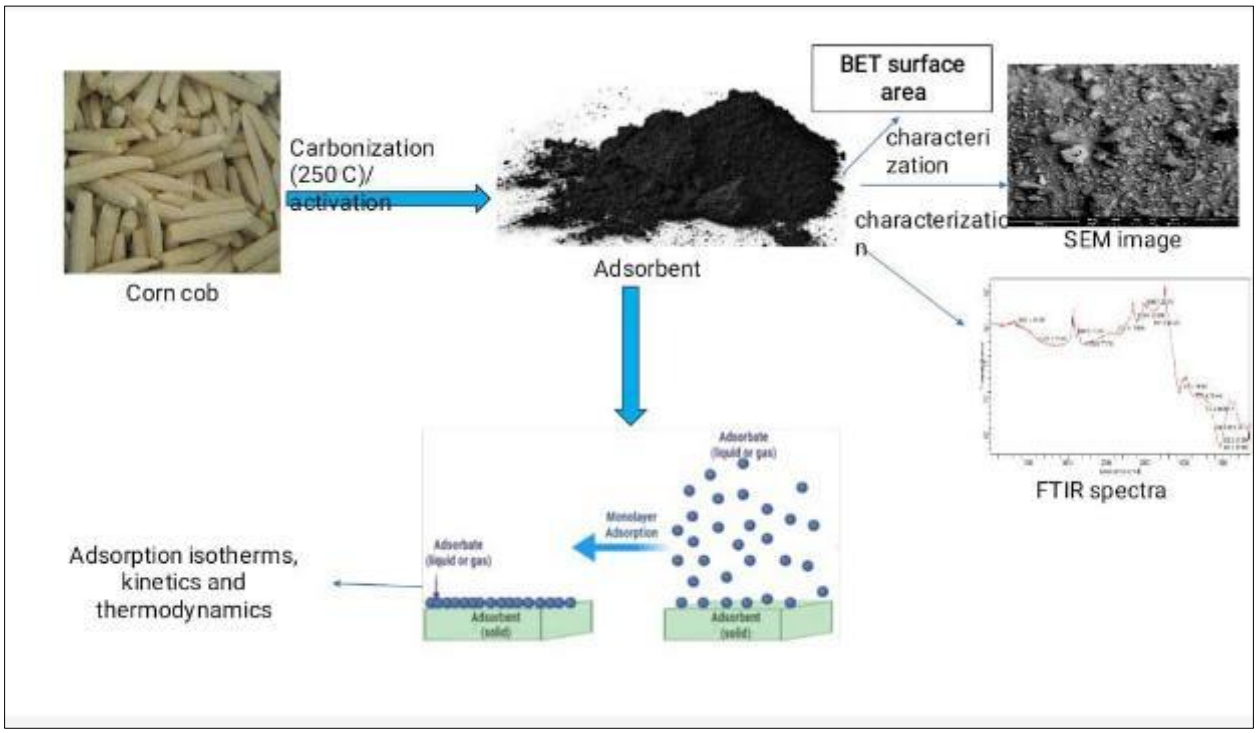

1. Introduction

Bisphenol A (BPA) $(CH_3)_2C(C_6H_4OH)_2$ is a chemical compound primarily used in the manufacturing of various plastics, resins, and epoxy materials [1]. However, its extensive use has led to contamination of water sources, posing significant risks to human health and the environment [2]. BPA causes diverse health issues among others are cancers [3], thyroid hormone disruption, normal cell function disruption, endocrine disturbances (EDCs), pancreatic β-cell function disruption, cardiovascular disease, liver damage, brain damage and sexual abnormalities [4]. It also affects tissue development, reproduction and behaviors [5]. BPA presence in the aquatic environment has raised a concern in the scientific and public community because of the diverse health issues it causes. Effective removal of BPA from aqueous solutions is crucial to mitigate its adverse effects.

Adsorption has emerged as a promising technology for removing BPA from water due to its simplicity, efficiency, and cost-effectiveness [6]. Various adsorbents have been explored, including activated carbon, zeolites, and biomass-based materials [1,4,6-8]. Among these, corn cob, a readily available and inexpensive agricultural waste, has shown potential as an adsorbent.

This study aims to investigate the adsorption of BPA onto hydrogen peroxide-modified corn cob (MCC) and unmodified corn cob (UMCC). The effects of modification on the adsorption efficiency at varying pH of the solution, adsorbent dosage, initial concentration, contact time and temperature, as well as the isotherm, kinetics, and thermodynamics of BPA adsorption were evaluated. The results of this study will provide insights into the feasibility of using MCC and UMCC as adsorbents for BPA removal from aqueous solutions. This work is a means of curbing water pollution from BPA contamination and a waste management practice of depleting corn cob from the waste streams.

2. Material and methods

2.1. Preparation of the unmodified (UMCC) and H_2O_2 modified corn cob (MCC) biochar

Corncobs collected from different dumpsites in Abakaliki town were cleaned off dirts and oven dried for at 105 ^{0}C for 2 hours. The cleaned dry corncobs were cut into smaller pieces and carbonized at 250 ^{0}C for 30 mins. The carbon obtained was ground and sieved using a standard sieve to obtain particles of size 0.75 mm. The resultant carbon is the UMCC. Part of the carbon was impregnated with 0.5 mol/dm^3 H_2O_2 in the ratio of 1:3 for 24 hrs, after which the carbon was

washed with distilled water until neutral [8]. The carbon was put in an oven at 105 ^{o}C for 2 hours and then put in the desiccator to cool down. The resulting biochar is the MCC. It was stored in a polythene bag for further analysis.

2.2. Characterization of the UMCC and MCC

The functional group of the UMCC and MCC was determined using FTIR (Cary 630 Agilent Technologies) machine at sample scan 30.8 resolution and within range of 4000 - 650 cm^{-1} by transmittance method. The morphology was analyzed using scanning electron microscopy SEM model Phenom ProX, at 200 μm, 15 kV and 400 magnifications. The BET surface area and pore volume was determined using a Micrometrics model ASAP 2020, 700VA made in USA. The average pore volume was calculated using the relationship:

$$\text{Average pore volume} = 4 \text{ x } \frac{total\ pore\ volume}{BET\ surface\ area} \quad \ldots\ldots\ldots\ldots\ldots\ldots (1)$$

2.3. Batch Adsorption Experiments

To measure the sorption kinetics and study time variation, 70 mg/L of BPA solution at pH 6 and dosage 0.06 g at 25 ^{o}C were used and time varied at 20, 40, 60, 90, 120 and 150 minutes. For sorption isotherms, 0.06 g of the biochar was added to different concentrations of BPA, 50. 60, 70, 90, 110, 130 mg/L, at pH 6, and the mixture equilibrated for 40 mins at 25 ^{0}C. Similar method was applied for pH varied at 3, 4, 6, 8, 9, 10, (with other conditions, 70 mg/L BPA, 40 mins and 0.06 g at 25 ^{o}C), adsorbent dosage 0.05 g, 0.06 g, 0.07 g, 0.08 g, 0.09 g, 0.10 g (at conditions 70 mg/L BPA, 40 mins and pH 6 at 25), and temperature varied at 25 ^{o}C, 40 ^{0}C, 55 ^{0}C, 65 ^{0}C. The mixtures were separated by filtration using Whatman No1 filter paper at the end of each experiment. The final concentrations of BPA in the solution were measured at maximum wavelengths of BPA (278 nm) using a double-beam UV/vis spectrophotometer (Shimadzu UV-160A). The percent removal of BPA was calculated using the relation in Equation 2:

$$(\%)\ \text{BPA removal} = \frac{\text{Initial concentration} - \text{final concentration}}{\text{Initial concentration}} \times 100 \quad \ldots\ldots\ldots\ldots\ldots\ldots\ldots (2)$$

The amount of equilibrium adsorption, q_e and q_t (mg/g) were calculated by:

$$q_e = \frac{c_i - c_e v}{w} \quad \ldots\ldots\ldots\ldots\ldots (3a)$$

$$q_t = \frac{c_i - c_t v}{w} \quad \ldots\ldots\ldots\ldots\ldots (3b)$$

where q_e and q_t are the absorption capacities at equilibrium and at time t(min) respectively, c_i and c_e are the concentrations of BPA at initial and equilibrium (mg/L) respectively, v is the volume of the solution (L), w is the weight of the adsorbent (g).

3. Results and conclusion

3.1. Characterization of the UMCC and MCC

The SEM images (Fig 1a and 1b), showed distinct morphological differences. The UMCC exhibited a relatively smooth and compact surface with fewer visible pores, while the MCC demonstrates a rougher texture with increased porosity, and noticeable surface etching, indicative of the oxidative effect of H_2O_2 treatment. The enhanced pore structure in the MCC suggests improved adsorption sites, supporting its higher efficiency in BPA removal.

The FTIR spectra of the UMCC and MCC (Fig 2a and 2b), revealed notable differences in functional group characteristics. The UMCC exhibited C≡C stretching (~2109 cm^{-1}), C-O stretching (~1982 cm^{-1}), and C-H bending (~872 cm^{-1}) associated with lignocellulosic materials, while the MCC showed, O-H stretching vibration (~3183 cm^{-1}), C-H stretching (~2885 cm^{-1}), which suggests higher hydrophilicity and improved adsorption properties, as well as enhanced hydroxylation, possibly due to oxidation by H_2O_2.

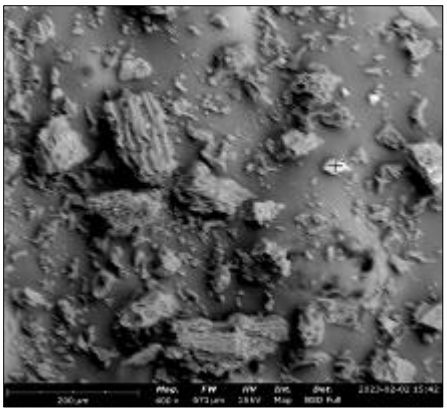

Figure 1a SEM image of UMCC

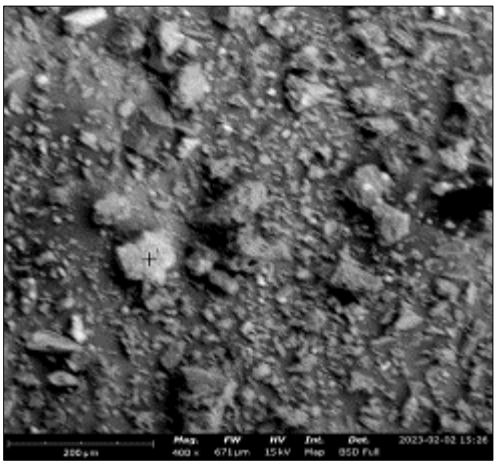

Figure 1b SEM image of MCC

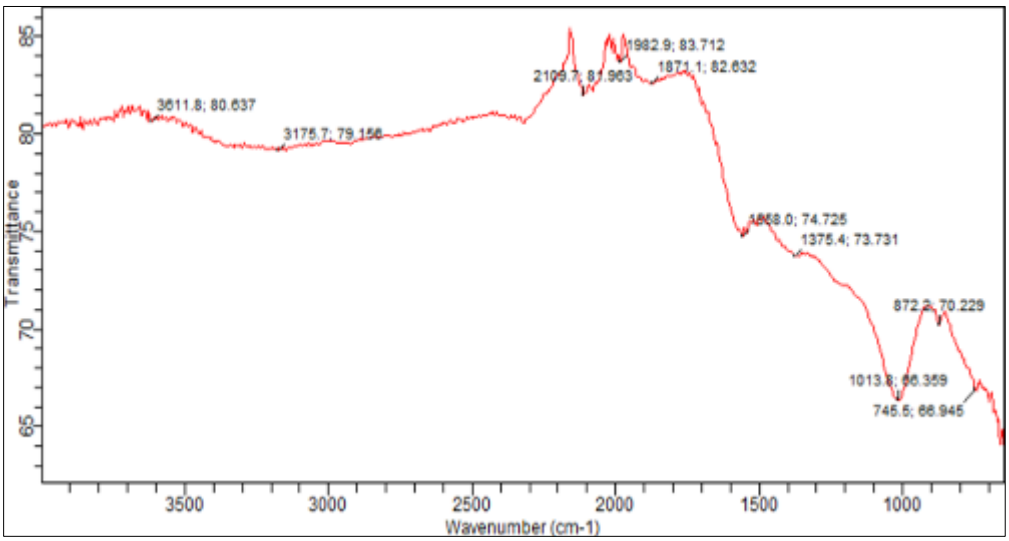

Figure 2a FTIR spectra of UMCC

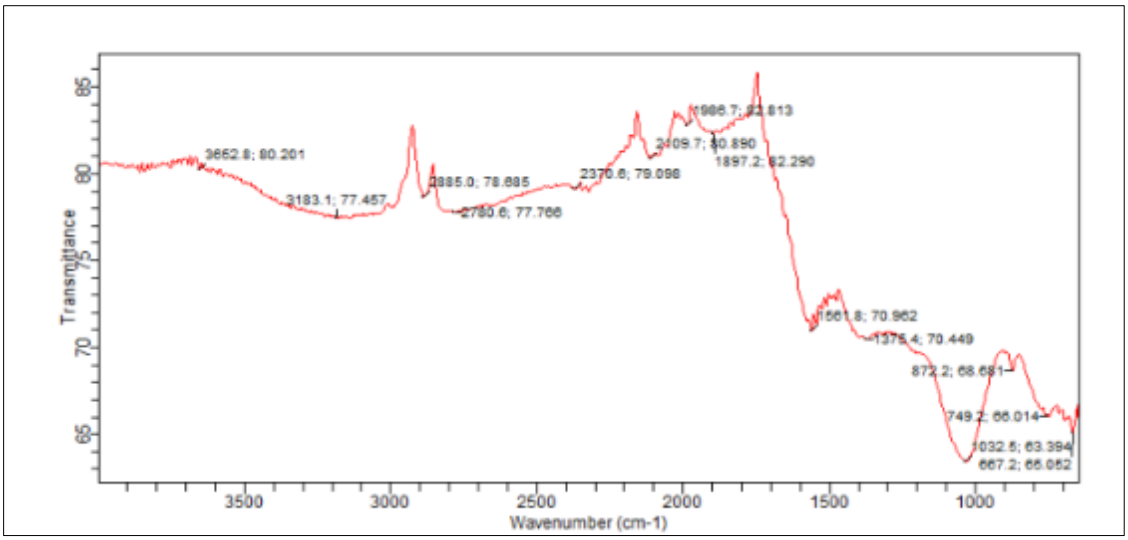

Figure 2b FTIR spectra of MCC

The BET surface area and average pore volume were 292 m^2/g and 0.484 cm^2/g (for UMCC), and 801.5 m^2/g and 2.86 cm^2/g (for MCC). The pore volume determines the rate at which the activated carbon can adsorb liquids; adsorption rate increases with increase in pore volume.

3.2. Adsorption experiments

3.2.1. Effect of contact time of MCC and UMCC on BPA Adsorption

The plot of percentage removal versus the contact time are shown in Fig 3. The adsorption equilibrium was established at 40 min at 86.25 and 60.30 % removal for both MCC and UMCC respectively. The removal was rapid at the first stage until the adsorption equilibrium was reached, thereafter the % removal remained constant from 40 - 150 min, due to saturated active sites of the adsorbent, which results to constant or decreased adsorption rate [9]. The trend also showed that the adsorption is in a state of dynamic equilibrium between the BPA desorption and adsorption after 40 min [10-11].

3.2.2. Effect of Initial Concentration of BPA on Adsorption by MCC and UMCC

Higher BPA removal yields were observed at lower concentrations (50 mg/L), with MCC having more efficient removal ability than UMCC (Fig 4). The saturation of the sorption sites on the adsorbent was observed as the concentration of the BPA increased. This is seen in the decrease in the % removal from 94.72 to 76.27 %, and 76.60 % to 48.30 % for MCC and UMCC respectively [9-10].

3.2.3. Effect of Solution pH on BPA Adsorption by MCC and UMCC

pH of the solution influences the adsorptive uptake of BPA because of its impact on both the surface-binding sites of the MCC and UMCC and the ionization process of the BPA molecule [12]. The H^+ ions on the surface of the adsorbents at these low pH causes electrostatic repulsion and competition between H^+ ions and BPA for the adsorption sites, preventing the adsorption of BPA ions onto adsorbent surface [13]. As the pH values increased, adsorbent surfaces were more negatively charged with subsequent attraction of BPA, resulting in favourable adsorption process for both MCC and UMCC, until a maximum was reached around pH 6 (Fig 5). Decrease in adsorption was observed at pH higher than 6. This may be attributed to the formation of soluble hydroxyl complexes [11]. MCC showed higher % removal of BPA (86.45 %) than UMC which has 60.48 % removal at pH of 6. All the adsorption experiments were conducted at this optimum pH value without adjustment.

3.2.4. Effect of Adsorbent Dosage of MCC and UMCC on BPA Adsorption

The removal efficiency of BPA increased with increasing adsorbent dosage for 70 mg/L initial BPA concentration for both UMCC and MCC (from 0.05 to 0.1 g). The higher the doses of the adsorbents, the more sorbent surface and pore volume will be available for adsorption [9,14]. This was seen in the increased BPA removal from 80.45 to 98.06 % and 58.38 to 75.41 % when the adsorbent concentration was increased from 0.05 to 0.1 g for MCC and UMCC respectively. The results also indicated MCC as more efficient in BPA removal than UMCC.

3.2.5. Effect of Temperature on BPA Adsorption by MCC and UMCC

The temperature effect on the adsorption of BPA on MCC and UMCC was investigated at 25, 40, 55 and 65 °C and results presented in Fig. 6. The results showed that the magnitude of adsorption is directly proportional to the temperature of the solution. The adsorption of BPA on MCC and UMCC increased from 86.45 % removal to 97.7 % removal, and 60.48 % removal to 73.14 % removal respectively, when temperature was increased from 25 to 65 °C. This is attributed to increase in the rate of diffusion of the adsorbate molecules across the external boundary layer and in the internal pores of the adsorbent particle, due to the decrease in the viscosity of the solution for highly concentrated suspensions when the temperature was increased [15].

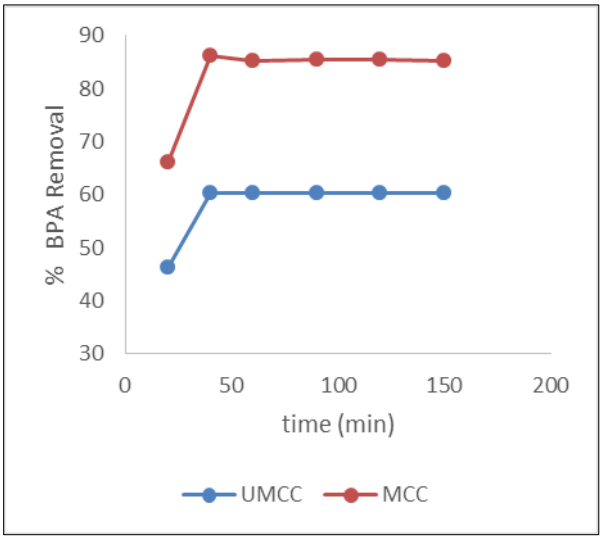

Figure 3 Effect of contact time on adsorption of BPA (T = 25 ^{0}C, pH = 6.0, adsorbent dosage = 0.06 g, Co = 70 mg/ L)

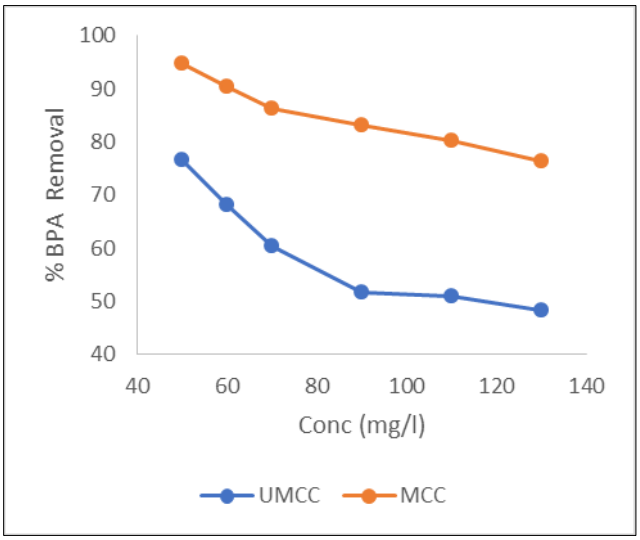

Figure 4 Effect of initial BPA concentration on adsorption by MCC and UMCC. (T = 25 ^{0}C, pH = 6.0, adsorbent dosage = 0.06 g, contact time = 40 min)

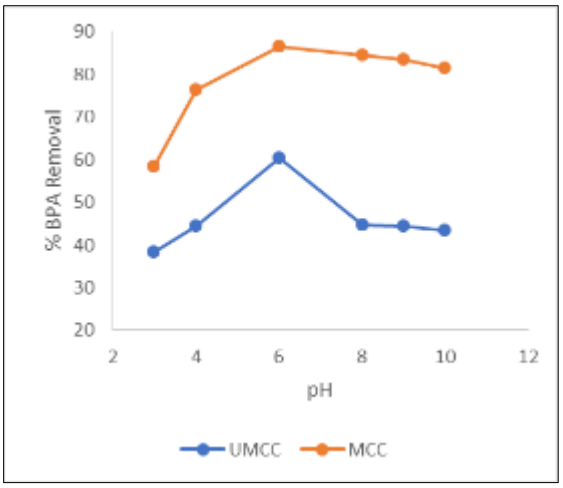

Figure 5 Effect of pH on the adsorption of BPA onto MCC and UMCC (T = 25 ^{0}C, Co = 70 mg/L, adsorbent dosage = 0.06 g, contact time = 40 min)

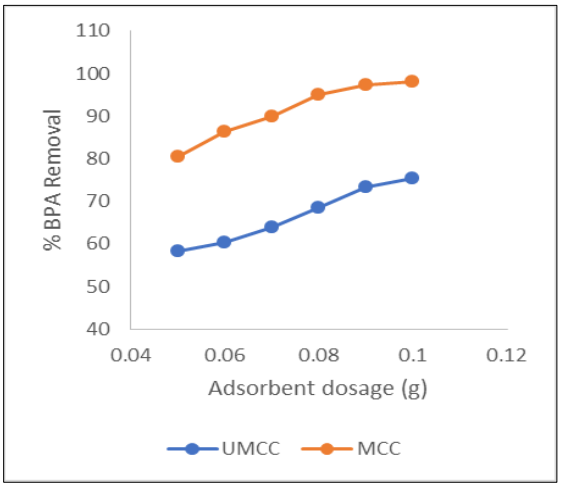

Figure 6 Effect of MCC and UMCC dosage on the adsorption of BPA (T = 25 ^{0}C, pH = 6.0, initial BPA Co = 70 mg/L, contact time = 40 min)

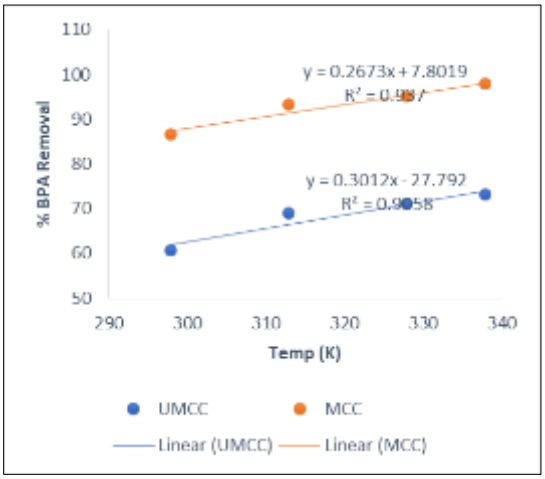

Figure 7 Effect of temperature on the adsorption of BPA onto MCC and UMCC biochar. (Co = 70 mg/L, adsorbent dosage = 0.06 g, pH = 6.0, contact time = 40 min)

3.3. Thermodynamic of BPA adsorption

In order to determine the process spontaneity for the BPA adsorption system by MCC and UMCC, plots of ΔG^o versus T (K) according to Equation 4 was drawn and changes in enthalpy (ΔH^0) and entropy (ΔS^0) were gotten from the intercept and slope of the plots by linear regression analysis (Fig.8). The standard Gibbs free energy ΔG^o at various temperatures (25 °C, 40 °C, 55 °C and 65 °C) were calculated using Equation 5

$$\Delta G^0 = \Delta H^0 - T\Delta S^0 \quad \text{..... (4)}$$

$$\Delta G^O = RT\ln K_D \quad \text{..... (5)}$$

where R is universal gas constant (8.314 J.mol^{-1}.K^{-1}), T is the temperature (K). The linear sorption distribution coefficient (K_D) is defined by $K_D = \frac{C_a}{C_e}$ were C_a and C_e are the equilibrium adsorbate concentration on the adsorbent (mg/g) and residual equilibrium adsorbate concentration (mg/g) respectively.

Thermodynamic parameters for the adsorption of BPA onto MCC and UMCC are presented in Table 1. The negative values of ΔG^o indicate that the adsorption of BPA onto MCC and UMCC is spontaneous in nature while the positive values of ΔH^o showed that the adsorption of BPA onto MCC and UMCC is endothermic in nature [16]. The negative values of ΔS^o suggest that there is decreased randomness at the solid/solution interface during the adsorption process of BPA on MCC and UMCC. This decreased randomness at the solid/solution interface during the adsorption process was observed more onto MCC than UMCC. Also, the adsorption of BPA onto MCC is more spontaneous than the adsorption of BPA onto UMCC. This makes MCC more efficient and better adsorbent for adsorbing BPA than UMCC.

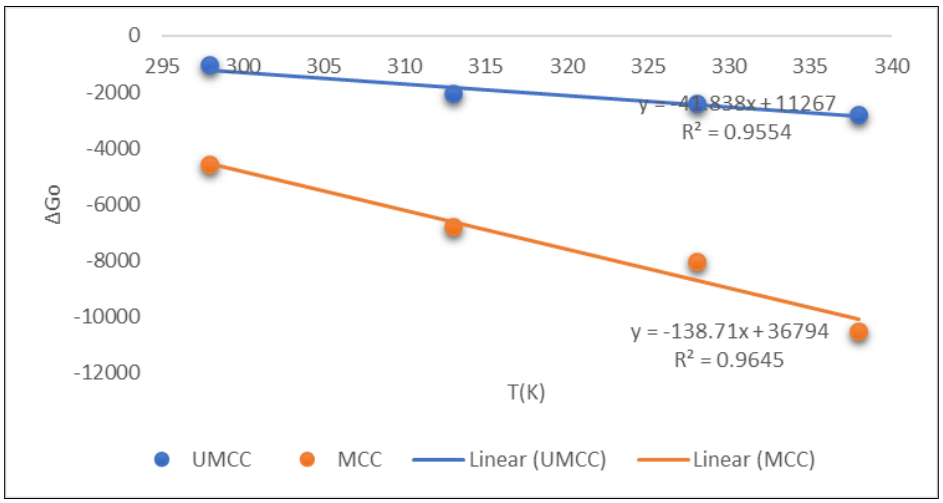

Figure 8 ΔG^o vs T for the adsorption of BPA onto MCC and UMCC

Table 1 Thermodynamic parameters for the adsorption of BPA onto MCC and UMCC

Adsorbents	ΔG^o (kJ/mol)				ΔH^o (kJ/mol)	ΔS^o (kJ/mol)
	298 K	313 K	328 K	338 K		
MCC	-4583.51	-6817.98	-8044.62	-10509.89	36794	-138.71
UMCC	-1065.36	-2055.80	-2427.02	-2810.13	11267	-41.838

3.4. Kinetics of BPA Adsorption by MCC and UMCC

The pseudo first-order and pseudo second-order kinetic models were used to study the kinetics of BPA adsorption by MCC and UMCC [17]. For pseudo first-order kinetic model, a plot of ln ($q_e - q_t$) versus t according to Equation 6 was constructed:

$$ln(q_e - q_t) = lnq_e - k_1 t \quad \text{..... (6)}$$

where q_t (mg/g) is the amount of adsorbed BPA on the adsorbent at time t, and k_1 (1/min) is the rate constant of first-order adsorption [11], q_e and k_1 can be determined from the intercept and slope of the plot, respectively.

The linearized form of the pseudo-second order kinetic expression is presented by Equation (7) [18]:

$$\frac{t}{q_t} = \frac{1}{k_2 q_e^2} + \frac{1}{q_e} t \qquad \text{..... (7)}$$

where k_2 (g.mol^{-1}.min^{-1}) is the rate constant of second order adsorption, q_e is the amount of BPA sorbed (mg/g) at equilibrium and at any time (t), qt (mg/g) is the amount of adsorbate retained at time t. The initial adsorption rate, h (mol.g^{-1}.Min^{-1}) is expressed as: $h = k_2 q_e^2$ (8),

the equilibrium adsorption capacity (q_e), and the second-order constants k_2(g.mol^{-1}.min^{-1}) were gotten experimentally from the slope and intercept of plot t/q_t versus t [16].

The validity of the kinetic models was tested by the magnitude of the regression coefficient R^2 gotten from the linear plots using Equations (6 -8). For the pseudo first-order model, the correlation coefficient is 0.0292 and 0.7206 for the MCC and UMCC respectively. These indicate a bad correlation, therefore; pseudo first-order model did not provide a good fit and the kinetic data not valid for this model. The correlation coefficient for the pseudo second -order model is 0.9982 and 0.9983 (Figure 9) for the MCC and UMCC respectively. These show a good correlation, therefore; pseudo second -order model provide a good fit and the kinetic data valid for this model. The pseudo second-order rate constants k_2, h, experimental equilibrium sorption capacity q_e (experimental) and calculated equilibrium sorption capacity q_e, (theoretical), at initial BPA concentrations of 70 mg/L on MCC and UMCC biochar are presented in Table 2. From Table 2, the q_e values calculated from the pseudo second order model for both biochar studied were in good agreement with the experimental qe values. Therefore, it can be deduced from these kinetic results that the rate-limiting step of the sorption of BPA on MCC and UMCC biochar may be chemisorption promoted by either covalent forces, through the exchange of electrons between the parties involved or valence forces, through sharing of electrons between adsorbent and adsorbate [19].

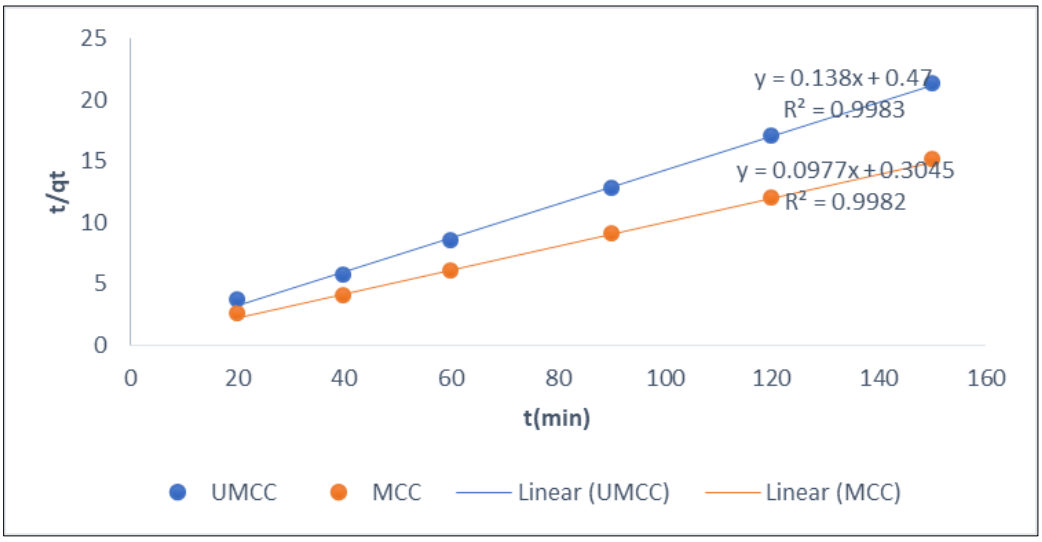

Figure 9 Pseudo second-order kinetics for adsorption of BPA onto MCC and UMCC at 25 °C (adsorbent dosage = 0.06 g/10 mL, pH = 6.0, contact time = 40 min.)

Table 2 Theoretical and experimental *qe* values, Pseudo second-order kinetic rate constants and the initial adsorption rate (*h*) for adsorption of BPA onto MCC and UMCC at initial BPA concentrations of 70 mg/L and temperature of 25 °C.

BIOCHAR	$q_{e,cal}$ (mg/g)	$q_{e,exp}$ (mg/g)	k_2 (mg/gmin)	H
MCC	10.06	10.24	0.031	0.308
UMCC	7.042	7.24	0.041	0.465

3.5. Isotherms of BPA Adsorption.

In order to find how the adsorption molecules distribute between the liquid phase and the solid phase when the adsorption process reaches an equilibrium state, the analysis of the isotherm data by fitting them to different isotherm models such as Langmuir, Freundlich and Temkin [20] adsorption isotherms. Table 3 showed the linear form of Langmuir, Freundlich and Tempkin equations, and parameters of the isotherms.

Table 3 Linear forms of the studied adsorption isotherms (Langmuir, Freundlich and Tempkin equations)

Langmuir	$\frac{C_e}{q_e} = \frac{1}{bQ_o} + \frac{C_e}{Q_o}$, where C_e is the equilibrium concentration of the adsorbate (mg/L); q_e is an amount of adsorbate in the adsorbent at equilibrium (mg/g); Q_o is the maximum monolayer coverage capacities (mg/g); b is the Langmuir constant (energy of sorption) which represents the affinity between the adsorbent and the solute (L/mg).
Freundlich	$\log q_e = \log K_f + \frac{1}{n \log C_e}$, *w*here K_f is the Freundlich constant or maximum adsorption capacity (mg/g); n is an empirical constant and 1/n is the intensity of adsorption.
Tempkin	$q_e = \frac{RT}{b_T} \ln K_t + \frac{RT}{b_T} \ln C_e$, *w*here K_t is equilibrium maximum binding energy (dm^3/g); b_T is a constant which is related to the heat of adsorption; R is the ideal gas constant; T is the absolute temperature

The fitted plots of the experimental data for each isotherm for adsorption of BPA onto MCC and UMCC are presented in Fig 7 (a –c)

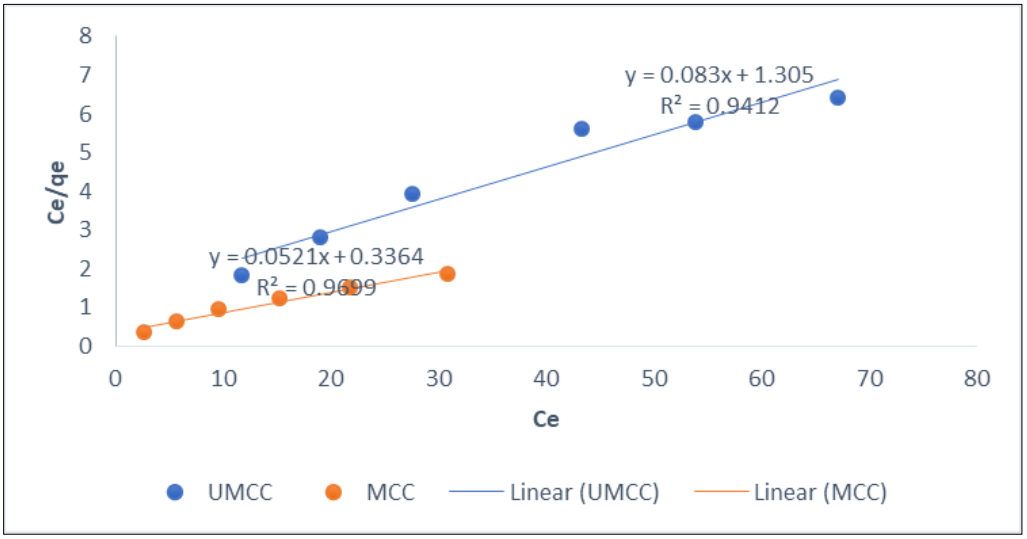

Figure 10a Fitted plots of the experimental data for Langmuir isotherm

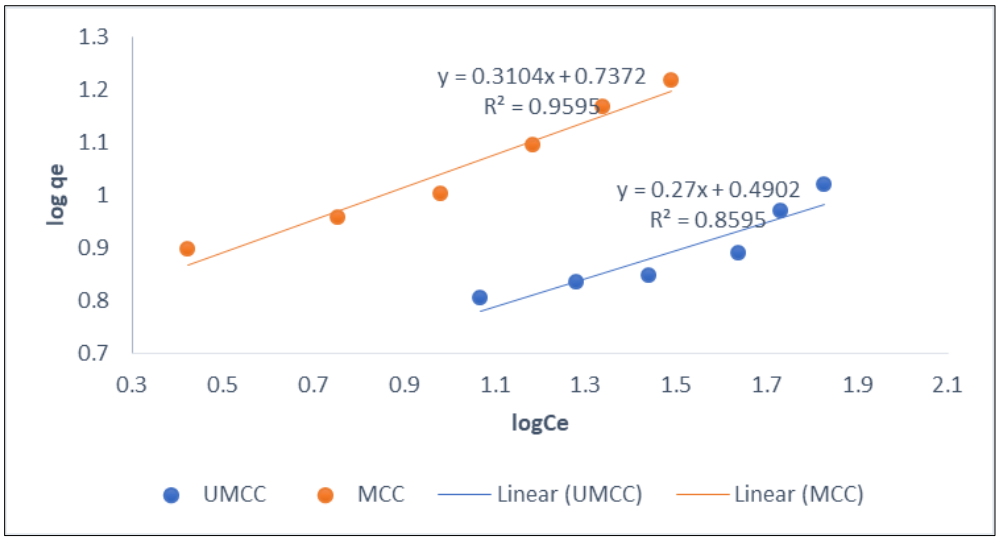

Figure 10b Fitted plots of the experimental data for Freundlich isotherm

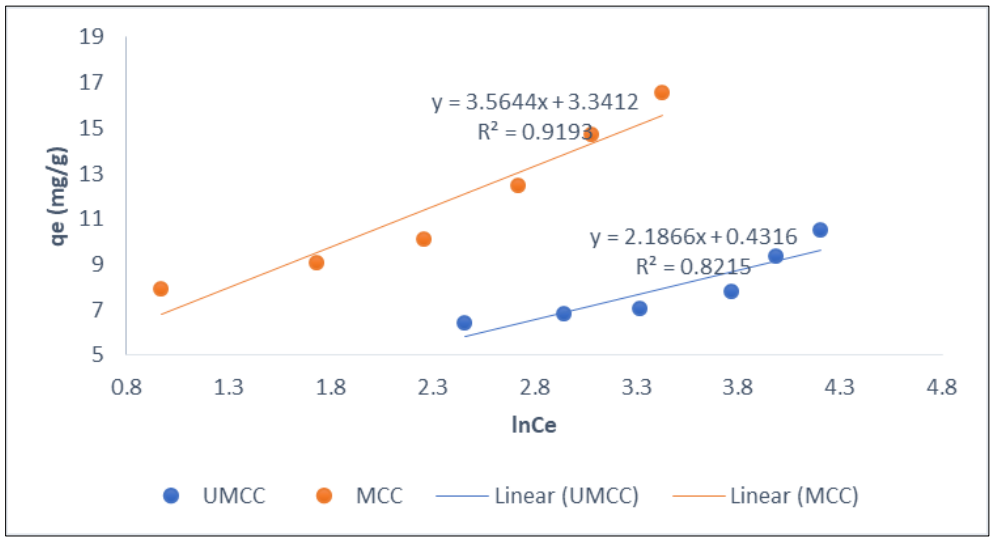

Figure 10c Fitted plots of the experimental data for Tempkin isotherm

The adsorption of BPA onto MCC and UMCC fits quite well into the Langmuir adsorption model. This shows that there is a homogenous distribution of active sites on the adsorbent surface, since the Langmuir equation assumes that the surface is homogenous [21]. The Q_0 and b for MCC is higher than that of UMCC. This is presented in Table 4. The higher value of b which represents the affinity between the adsorbent and the solute indicates a favorable adsorption process with MCC than UMCC. The essential characteristics of Langmuir isotherm which can be expressed by a dimensionless constant called the separation factor or equilibrium parameter R_F according to Equation 8 presented in Table 4 are in the range of $0 < R_F < 1$. This showed that the adsorption processes were favourable [22-24].

$$R_F = \frac{1}{1+bC_0} \quad \text{..... (9),}$$

where b is the Langmuir constant and C_o (mg/L) is initial BPA concentration.

Adsorption of BPA onto MCC also showed good fits into Freundlich and Tempkin isotherms, while the adsorption with UMCC biochar shows fairly good fits into Freundlich and Tempkin isotherm (Fig 7a–c). As presented in Table 5, The values of the exponent $1/n$ (i.e. intensity of adsorption or surface heterogeneity) unto MCC and UMCC biochar were in the range of $0 < 1/n < 1$, indicating favourable adsorption [21]. The maximum adsorption capacity, K_F of adsorption of BPA by MCC is higher than K_F of adsorption of BPA by UMCC. Also, the equilibrium maximum binding energy of sorbate to the sorbent, K_t is higher in adsorption of BPA by MCC than K_t of adsorption of BPA by UMCC biochar. The b_T which is

related to the heat of adsorption is lower for adsorption by MCC than b_T for adsorption by UMCC. This shows that lesser energy is required to adsorb BPA by MCC than the energy required to adsorb BPA by UMCC. It can be inferred from this that the adsorption of BPA by MCC is more efficient than adsorption of BPA by UMCC.

Table 4 Isotherm constants for BPA onto MCC and UMCC

Adsorption Isotherms	**MCC**	**UMCC**
Langmuir isotherm		
Q_0 (mg /g)	19.194	12.048
b (L/g)	1.549	0.064
R_L	0.0091	0.182
R^2	0.9699	0.9412
Freundlich isotherm		
K_f (L/g)	5.46	3.092
1/n	0.3104	0.27
R^2	0.9595	0.8595
Tempkin isotherm		
K_T (L/g)	2.555	1.218
b_T	69.509	113.307
R^2	0.9193	0.8215

4. Conclusion

In this work, low-cost adsorbents were synthesized and used to carry out the isotherm, kinetics and thermodynamic studies on the adsorption of BPA from aqueous solution. The efficiency of the adsorbents (UMCC and MCC) was compared in order to determine which material has higher adsorption capacity, faster kinetics and better removal performance. Batch experiment on variation of pH, temperature and contact time revealed that the optimum pH value for BPA adsorption was observed at pH 6.0 for both MCC and UMCC, adsorption increased with increase in temperature, and that the equilibrium of the BPA adsorption was reached within 40 min The dimensionless separation factor (R_L) calculated showed that MCC and UMCC can be used for removal of BPA from aqueous solutions with MCC as the more efficient adsorbate removal. The adsorption of BPA followed Langmuir isotherm, indicating homogenous (monolayer) adsorption nature. Validity of the kinetic models tested by the magnitude of the regression coefficient R^2, indicated that the kinetics followed pseudo-second-order kinetic model. The negative value of ΔG^o and positive value of ΔH^o gotten from the thermodynamic study showed that the adsorption process of BPA with MCC and UMCC is spontaneous and endothermic in nature. Corn cob is available everywhere and H_2O_2 used for modification is inexpensive. We therefore recommend MCC to be used as an alternative to costly adsorbents used for BPA removal in wastewater treatment processes. This can help to create value added products from waste materials, promoting circular economy.

Compliance with ethical standards

Disclosure of conflict of interest

The authors declare that there are no conflicts of interest.

References

[1] Zhao Z, Fu D, Ma Q. Adsorption characteristics of Bisphenol A from aqueous solution onto HDTMAB-modified Palygorskite. Separation Science and Technology. 2014; 49: 81-89. doi: 10.1080/01496395.2013.818693.

[2] Chen M.Y, Lyke M, Fujita M. Acute toxicity, mutagenicity, and erogenicity of Bisphenol A and other Bisphenols. Environmental Toxicology. 2002; 17: 80-86.

[3] Rubin, B.S. Bisphenol A: An endocrine disruptor with widespread exposure and multiple effects. Journal of steroid biochemical molecular biology. 2011;127: 27-34.

[4] Dehghani M. H, Mahvi A. H, Rastkari N, Saeed R, Nazmara S, Iravani E. Adsorption of Bisphenol A (BPA) from aqueous solutions by carbon nanotubes: kinetic and equilibrium studies. Desalination and water treatment. 2015; 54: 84-92. doi: 10.1080/19443994.2013.876671

[5] Wolstenholme J.T, Rissman E.F, Connelly J.J. The role of Bisphenol A in shaping the brain, epigenome and behavior. Hormonal behavior. 2011; 59: 296-305

[6] Liu G, Ma J, Li X, Qin Q. Adsorption of Bisphenol A from aqueous solution onto activated carbons with different modification treatments. Journal of hazardous materials. 2009; 164: 1275-1280.

[7] Seyhi B, Drogui P, Buelna G, Blais J.F. Modeling of sorption of Bisphenol A in sludge obtained from a membrane bioreactor process. Chemical engineering journal. 2011; 172: 61-67.

[8] Eze N. O, Vincent F. U, Ogbonna O. N, Nwidembia P. O, Solomon C, Oti W. O. Acid and alkaline pretreatment of biochar and their effect on removal of Bisphenol A from aqueous solution. Journal of chemical society of Nigeria. 2024; 49(5): 792-802

[9] Eze N. O, Ejimofor S. A, Onuegbu T. U. Equilibrium and kinetic studies of liquid phase adsorption of methylene blue onto phosphoric acid modified bambaranut shell, Acta Chemica Malaysia. 2021; 5 (2): 42- 52. doi:10.2478/acmy-2021-0007

[10] Kumar P.S, Ramalingam S, Senthamarai C, Niranjanaa M, Vijayalakshmi P, Sivanesan S. Adsorption of dye from aqueous solution by cashew nut shell: studies on equilibrium isotherm, kinetics and thermodynamics of interactions. Desalination. 2010; 261: 52-57

[11] Farman A, Nisar A, Iram B, Amir S, Shahid N, Zarshad A, Syed M. S, Hafiz M. N, Muhammad B. Adsorption isotherm, kinetics and thermodynamic of acid blue and basic blue dyes onto activated charcoal. Case studies in chemical and environmental engineering. 2020; 2. https://doi.org/10.1016/j.cscee.2020.100040

[12] Temesgen F, Gabbiye N, Sahu O. Biosorption of reactive red dye (RRD) on activated surface of banana and orange peels: economical alternative for textile effluent. Surfaces and interfaces. 2018; 12: 151-159.

[13] Lin Q, Gao M, Chang J, Ma H. Adsorption properties of crosslinking carboxymethyl cellulose grafting dimethyl diallyl ammonium chloride for cationic and anionic dyes. Carbohydr. Polym. 2016; 151: 283-294.

[14] Fufa F, Alemayehu E, Lennartz B. Sorptive removal of arsenate using termite mound. Journal of Environ. Manage. 2014; 132: 188-196. http//dx.doi.org/10.1016/j.jenvman2013.10.018

[15] Yu L J, Shukla S. S, Dorris K. L, Shukla A, Margrave J. L. Adsorption of chromium from aqueous solutions by maple sawdust. Journal of hazardous materials. 2003; 100: (1-3) 53-63. https://doi.org/10.1016/s0304-3894(03)00008-6

[16] Ebelegi A N, Ayawei N, Wankasi D. Interpretation of adsorption thermodynamics and kinetics. Open journal of physical chemistry. 2020; 10:166-182

[17] Yan L, Liu Y, Zhang Y, Liu S, Wang C, Chen W, Liu C, Chen Z, Zhang Y. ZnCl2 modified biochar derived from aerobic granular sludge for developed microporosity and enhanced adsorption to tetracycline. Bioresource Technology. 2020; 297: 122381

[18] Ademiluyi F. T, Nze J. C. Sorption characteristics for multiple adsorptions of heavy metal ions using activated carbon from Nigerian bamboo. Journal of Materials Science and Chemical Engineering. 2016; 4: 39-48

[19] Franca A.S, Oliveira L S, Ferreira M E. Kinetics and equilibrium studies of methylene blue adsorption by spent coffee grounds. Desalination. 2009: 249: 267-272. Doi. 10.1016/j.desal.2008.11.017

[20] Zhang Z, Li H, Liu H. Insight into the adsorption of tetracycline onto amino and amino-Fe3+ functionalized mesoporous silica: Effect of functionalized groups. Journal of environmental science. 2018; 65: 171-178.

[21] Sampranpiboon P, Charnkeitkong P, Feng X. Equilibrium isotherm models for adsorption of Zinc (II) ion from aqueous solution on pulp waste. WSEAS Transaction on Environment and Development. 2014; 35-47.

[22] Karagöz S, Tay T, Ucar S, Erdem M. Activated carbons from waste biomass by sulfuric acid activation and their use on methylene blue adsorption. Bioresource technology. 2008; 99(14): 6214-6222. https://doi.org/10.1016/j.biortech.2007.12.019

[23] Ajenifuja E, Ajao J, Ajayi J. Adsorption isotherm studies of Cu (II) and Co (II) in high concentration aqueous solutions on photocatalytically modified diatomaceous ceramic adsorbents. Applied water science. 2017; 7(7): 3793-3801

[24] Paudel S, Shrestha B. Adsorptive removal of iron (II) from aqueous solution using raw and charred bamboo dust. International journal of advanced social sciences. 2020; 3(2): 27-35.